Hindawi Publishing Corporation
International Journal of Antennas and Propagation
Volume 2012, Article ID 106296, 8 pages
doi:10.1155/2012/106296

Research Article

EBG Size Reduction for Low Permittivity Substrates

Gonzalo Expósito-Domínguez,[1] José Manuel Fernández-González,[1] Pablo Padilla,[2] and Manuel Sierra-Castañer[1]

[1] *Radiation Group, Department of Signals, Systems and Radio Communications, University of Madrid, 28040 Madrid, Spain*
[2] *Department of Signal Theory, Telematics and Communications, University of Granda, Granda 18071, Spain*

Correspondence should be addressed to Gonzalo Expósito-Domínguez, gexposito@gr.ssr.upm.es

Received 3 September 2012; Accepted 13 December 2012

Academic Editor: Eric Lheurette

Double layer and edge-location via techniques are combined for electromagnetic band gap (EBG) size reduction. The study of the required number of elements and their dimensions is carried out in order to suppress the surface wave propagation modes and consequently to reduce the mutual coupling between radiating elements in low-permittivity substrates. By applying these techniques, the size of the EBG mushroom is reduced by 30%; however, the bandwidth operation maintains its value, and these structures can be integrated between radiating elements in broad bandwidth antennas.

1. Introduction

Low-profile integrated antennas are demanded to be small [1]. In order to reduce the size of the antenna or to increase the working frequency band, high-permittivity substrates are used. However, with this type of substrates, surface wave propagation modes are enhanced, and there is strong mutual coupling [2]. In array antennas, the separation between elements should not be higher than $0.8\,\lambda_0$ in order to avoid grating lobes and to get high directivity. This last condition regarding the separation between radiating elements increases the mutual coupling because the elements are closer and they have stronger interaction.

The most common mutual coupling reduction techniques are cavity structures [3], nonuniform feeding distribution [4], unequally space distribution [5], and defected ground plane (DGP) [6], but lately, (EBG) structures are being used. The introduction of several rows of EBG structures between two printed antennas has been proved to increase the isolation [7]. However, when low-permittivity substrates are used in order to enhance the radiation efficiency, the size of the printed antenna elements increases, and the available space between radiating elements is not sufficient to introduce the necessary number of EBG rows.

Patch antennas are found to have very strong mutual coupling due to the severe surface waves on thick and high-permittivity substrates. In the literature, it can be found a variety of works which apply metamaterials for the reduction of this effect. In [7], four rows of EBG mushrooms are inserted between the patch antennas in $\epsilon_r = 10.2$ and thickness ($h = 2\,\text{mm}$) substrate. With this configuration, 8 dB of mutual coupling reduction is obtained. In [8], different substrates are combined; radiating elements are suspended over a thick foam layer in order to increase the bandwidth, and meanwhile, EBG structures are printed in a thin high-permittivity substrate for size reduction and surface wave suppression. In [9], by using edge-located vias, the size of mushroom-type EBG is reduced by 20%. Among other strategies, in [10], a fork shape is used. The area occupied by the fork-like structure is less than 25% of the mushroom-like structure. Besides, microelectromechanical systems (MEMS) are used, and reconfigurable stop band is obtained. Another studied technique is the use of metal strips. Basically, the idea is to combine the EBG concept with soft surfaces. A comparison of mushroom-type EBG surfaces and corrugated and strip-type soft surfaces is shown in [11]. This stripe-type is used in [12, 13] to reduce mutual coupling. Finally, dual band planar soft surfaces are developed in [14]; two sizes of

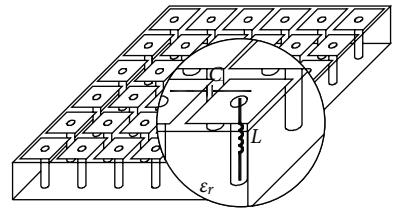

Figure 1: High impedance surface and its model with parallel resonant LC circuit. The substrate is transparent in order to get better visualization of metallic vias.

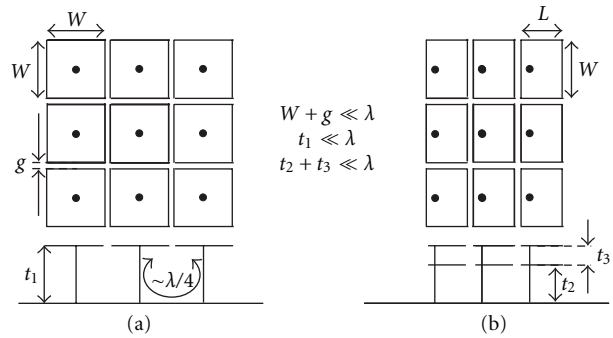

Figure 2: Layer and top views of traditional EBG structures (a) and multilayered F structure (b).

strips are mixed in order to get dual forbidden band. Thanks to its frequency selective feature, these EBG structures can be used as a filter. By applying three elements as a ground plane for a microstrip line, in [15], isolation levels higher than 55 dB in the first frequency band (2.1 GHz) and 40 dB in the second one (2.45 GHz) are achieved.

The main goal of this work is to combine multilayer technique with edge-location via [16] to find a new solution for EBG size reduction when using thick and low-permittivity substrates (in this case mushroom type [17]). By applying multilayered structure, different shapes, and edge-location via, the effective size is reduced by 30%, and EBG structures fit in between printed antennas. This paper is organized as follows. An overview of the EBG materials theory is provided in Section 2. Section 3 is devoted to study different solutions to obtain surface wave suppression characteristics. In Section 4, different EBG topologies, sizes, and number of periods are simulated and constructed in order to reduce the size of the mushroom to place it between radiating elements. Finally, in Section 5, the conclusions are drawn.

2. EBG Theory Fundamentals

EBG technique appears as an application of truncated frequency selective surfaces (FSSs) [17]. These structures consist of array patches printed in a substrate, which are short circuited to the ground plane with vias and can be visualized as mushrooms protruding from the surface, as shown in Figure 1.

When the period is small compared to the wavelength of interest, it is possible to analyze the material as an effective medium with a surface impedance (metamaterial with electrical properties [18]). These "mushrooms" present very high impedance values for vertical and horizontal propagation modes at certain frequencies. In Figure 2, on the left hand side, traditional mushrooms are shown, and meanwhile, on the right hand side, a multilayered mushroom structure is presented.

The behavior of this structure is similar to an LC circuit in (1). Below the resonance frequency, the surface is inductive, while above resonance frequency, the surface is capacitive. Consider

$$\omega_0 = \frac{1}{\sqrt{LC}}. \tag{1}$$

Nearby ω_0, the surface impedance (Z_s) is much higher than the impedance of free space, as (2) depicts. Therefore, no vertical or horizontal propagation modes are allowed. Consider

$$Z_s = \frac{j\omega L}{1 - \omega^2 LC}, \tag{2}$$

where the capacitance C is provided by the proximity of the metal plates, according to (3) [19] as follows:

$$C = \left[\frac{w\varepsilon_0(\varepsilon_{\text{eff}})}{\pi}\right]\cosh^{-1}\left(\frac{2w}{g_0}\right), \tag{3}$$

and the inductance L (4) is related to the thickness of the structure, because its value is due to the length of the via as follows:

$$L = \mu_0 t. \tag{4}$$

Analytically, it can be noticed that the band gap operation band is proportional to $\sqrt{L/C}$. Thus, for a fixed separation of

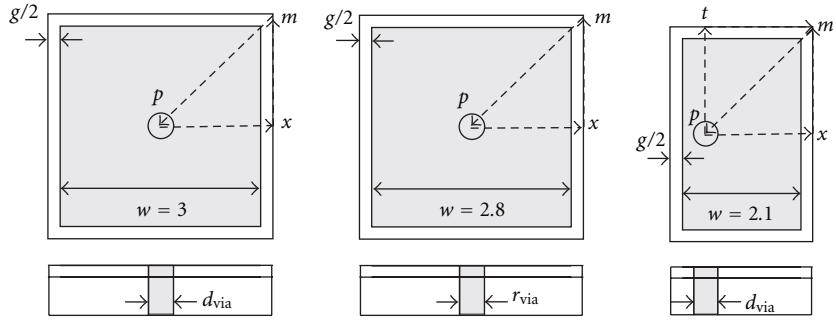

(a) Original mushroom (b) Double layer mushroom (c) Double layer and edge-location via mushroom (F shape)

Figure 3: Unit cell scheme for eigenmode solutions.

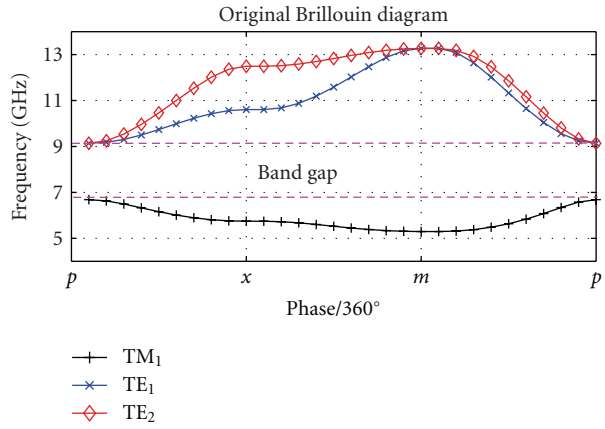

Figure 4: Brillouin diagram for original mushrooms.

the metal plates, the value of the capacitance is set, and the working bandwidth can be increased by increasing the length of the via and therefore the thickness of the substrate, which is adequate for wideband antennas.

Finally, EGB structures can be seen as bend corrugations, where the length of the corrugation is the sum of the via and the patch multiplied by two, as it is depicted in Figure 2. The band gap operation of the corrugations starts and finishes when the length is similar to $\lambda/4$ and $\lambda/2$, respectively, which yields a frequency octave [20].

3. Surface Wave Suppression

Thanks to the high surface impedance, horizontal or vertical modes are not allowed in the mushroom structures at certain frequencies. In order to find the allowed frequencies for each wave vector, a single unit cell with periodic conditions is simulated. The x-axis represents the dimensions inside the unit cell in which the boundary conditions are fulfilled at certain frequencies for the transmission modes of the structure. In Figures 3(a) and 3(b), the unit cell is symmetric with respect to the via; thus, only three traces have to be computed. However, for the F shape case in Figure 3(c), the EBG structure does not have the same dimensions in x and y. Therefore, five traces have to be analyzed to describe all the possible propagation modes for these boundary conditions.

All the studied structures are developed in a low-permittivity substrate $\varepsilon_r = 2.17$ and thickness of 1.143 mm. For the traditional mushroom, the size of the original patch in X band (7.25–8.4 GHz) is 3 mm × 3 mm, while on the other hand, for double layer mushroom 2.8 mm × 2.8 mm size is used. For this last configuration, two stacked substrates of 0.762 mm and 0.381 mm thickness are used.

The electric field is described in terms of an eigenvalue equation, which is solved numerically. In Figures 4, 5, and 6, the mode solutions that satisfy the boundary conditions are shown. The abscissa value represents the wave number which fulfils the requirements at a certain frequency. The lowest line is the TM mode, while the second and third lines are TE modes. A frequency band gap (dashed lines), in which the surface does not support surface wave propagation of either polarization, horizontal nor vertical, extends from the top of the TM band to the point where TE band crosses the light line. The comparison between original shape and double layer mushrooms yields the result of 2 GHz bandwidth for the original shape and 1.2 GHz for the multilayer solution.

In this work, the combination of multilayer structure [17] and edge-location via [16] for mushroom size reduction

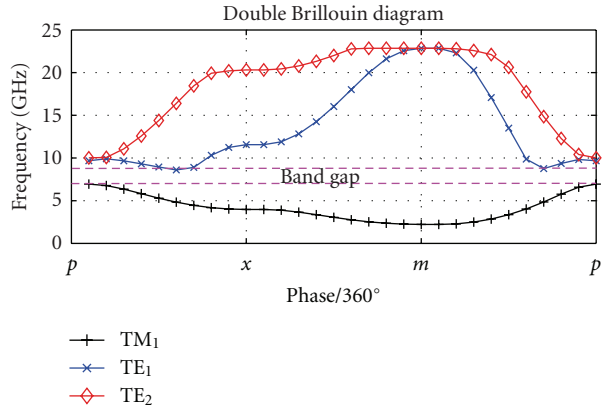

Figure 5: Brillouin diagram for double layer mushrooms.

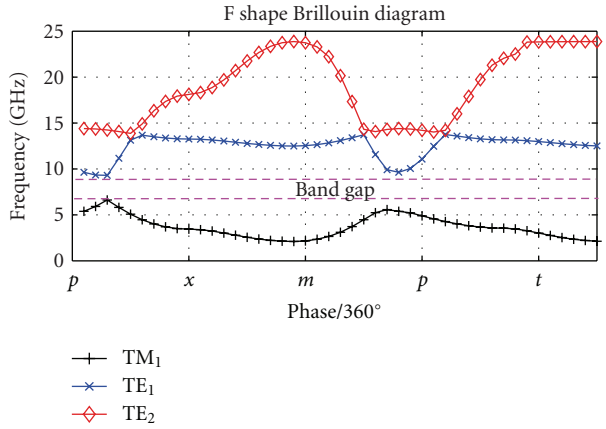

Figure 6: Brillouin diagram for F shape mushrooms.

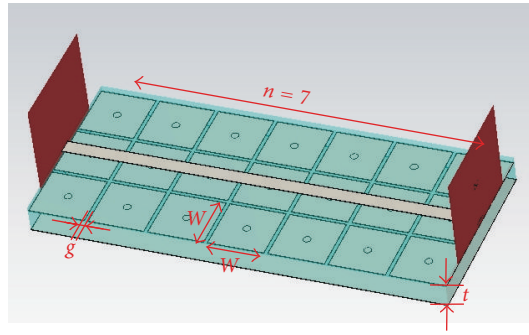

Figure 7: Simulation scheme for S_{21} analysis.

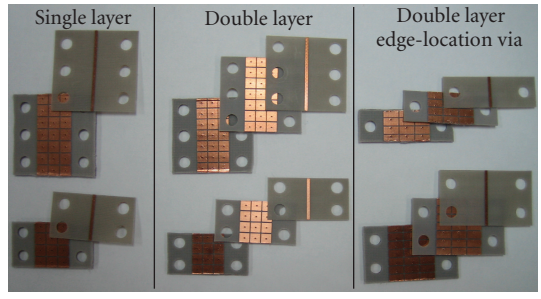

Figure 8: Samples of single and multilayered EBG mushrooms with different shapes and number of elements.

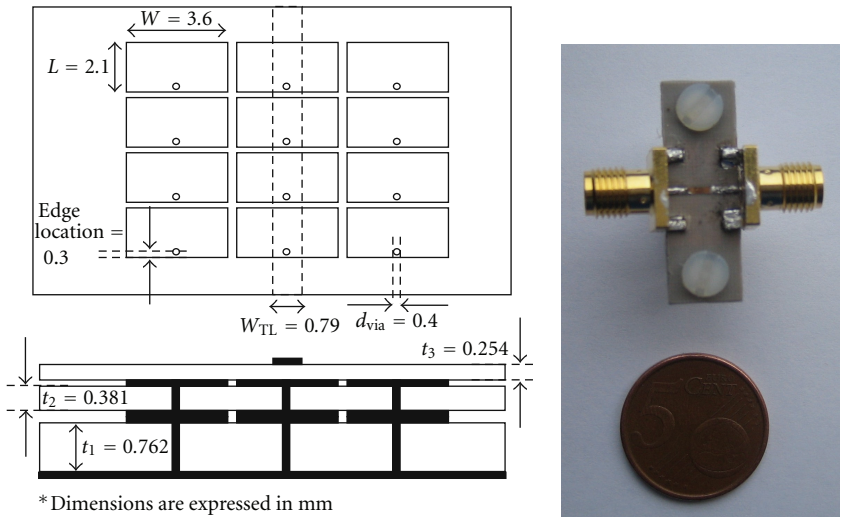

(a) Schematic (b) Prototype

FIGURE 9: Multilayered mushroom with rectangular shape, 4 elements and edge-located via (F-shape).

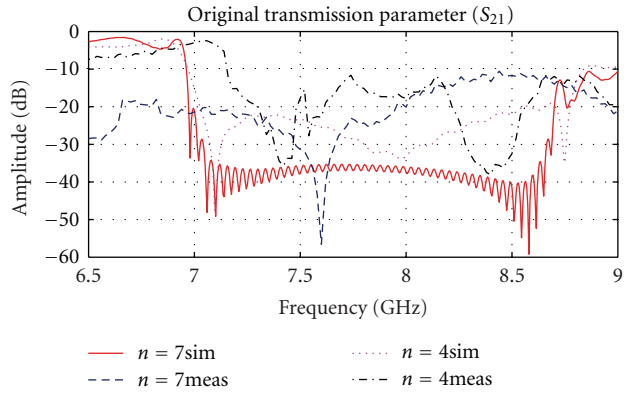

FIGURE 10: Transmission parameters (S_{21}) for original mushrooms.

is discussed. In order to keep the frequency working band (15%) and radiation efficiency, the same substrate ($\varepsilon_r = 2.17$ and thickness of 1.143 mm) is used. As long as the inductance depends on the substrate thickness, which is fixed already, the only available parameter is the capacitance C. In order to increase this parameter, a multilayered structure with edge-location via is presented. The dimensions of the patches are 2.1 mm × 3.6 mm (this value means 30% size reduction in the critical direction). The Brillouin diagram for this configuration is presented in Figure 6. In this case, the bandwidth keeps its value, but significant size reduction is noticed.

4. Mutual Coupling Reduction

The size of the mushroom patches and the necessary number of periods for mutual coupling reduction are higher than the available space between radiating elements for low-permittivity substrates. For example, for steering arrays antennas, separation must not be higher than 0.6 λ_0 in order to avoid grating lobes. To study this effect, a simulation scheme for S_{21} analysis is proposed in Figure 7. In this simulation, different topologies (original, double, or F shape), size of the mushroom w, gap size g, and number of elements n are tested in order to obtain the surface wave suppression behavior.

In order to validate the whole process, prototypes of four and seven rows are built. Six prototype transmission lines (TLs) with EBG ground plane are mounted in Figure 8. On the left hand side, the two circuits are single layered, the two circuits in the middle are double layered, and the last two circuits on the right hand side combine double layer with edge-location via (F shape).

All the substrates used have permittivity of $\varepsilon_r = 2.17$. However, four different thickness values are used. The TLs impedance is 50 Ω, and those TLs are printed in a 0.254 mm thick substrate. Mushroom in single layer case are printed in a 1.143 mm thick substrate, while in double layer case is printed in 0.762 mm (bottom layer) and 0.381 mm thick (upper layer) substrates. Therefore, total thickness value maintains its value as it can be seen in Figures 9(a) and 9(b).

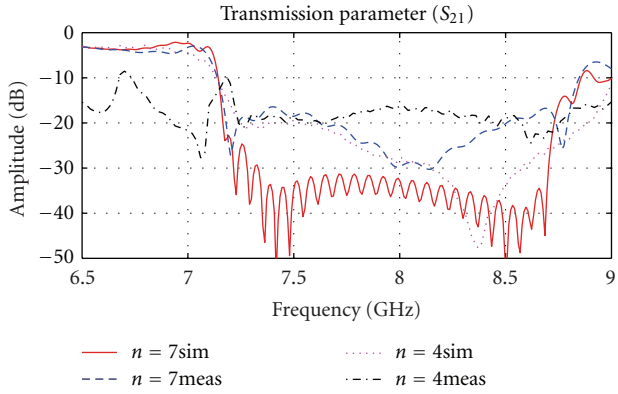

Figure 11: Transmission parameters (S_{21}) for double layer mushrooms.

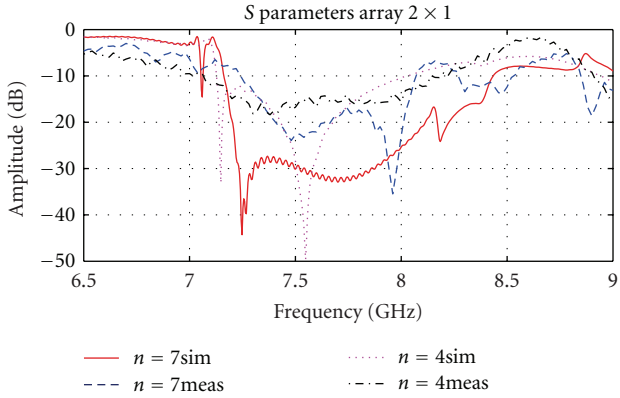

Figure 12: Transmission parameters (S_{21}) for F shape mushrooms.

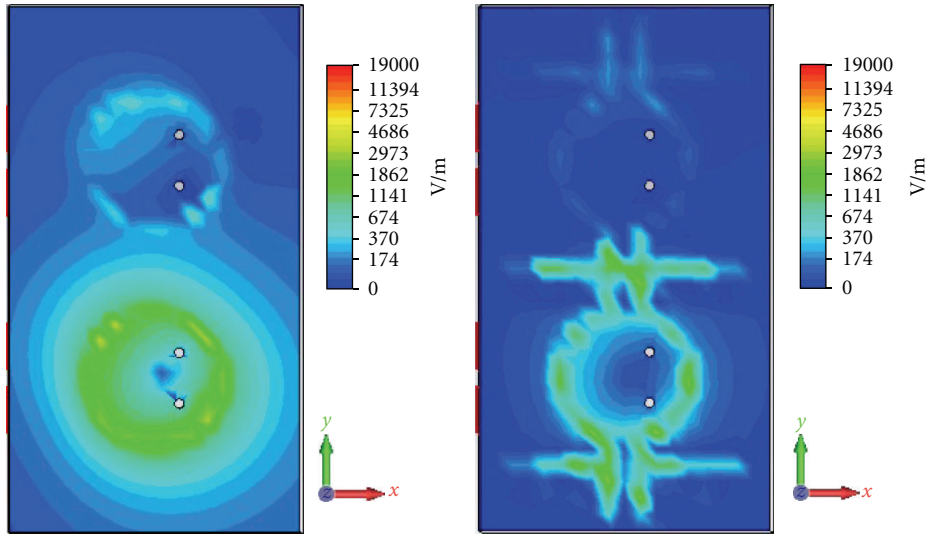

(a) Without EBG structures (b) With EBG structures

Figure 13: $|E|$ field simulation of two round patches with dual circular polarization.

In Figures 10, 11, and 12, comparisons between the simulated structures and the measured prototypes are shown. Difficulties due to the small size of the circuits (size circuit approximately 1 cm) add some differences between simulations and measurements. However, the overall behavior of an LC filter in a certain frequency band is observed. It can be noticed, comparing the figures, that traditional mushrooms have larger frequency operation band than F shape mushrooms. However, F shape ones keep fulfilling the bandwidth and isolation requirements.

Finally, the tradeoff solution between isolation and available space is carried out, being the necessary number of periods for surface wave suppression: $n = 4$. In Figures 9(a) and 9(b), the chosen topology is shown. With final dimensions of 2.1×3.6 mm, four elements, double-layered structure and edge-location via, fulfil the requirements of available space (10.2 mm) between 2 printed antennas separated $0.6\,\lambda_0$ in $\varepsilon_r = 2.17$ and 1.143 mm thick substrate. A bandwidth operation in X band, from 7.1 GHz to 8.2 GHz (15%) and 10 dB of isolation, is obtained.

In order to prove this solutions four rows of double-layered edge-located via, EBG mushrooms are introduced between two round patches with double circular polarization. The radiating elements are integrated in the same substrate, and they are circular polarized. The elements are fed by a 90°/3 dB branch line coupler in order to get the double circular polarization.

In Figure 13(a), $|E|$ field simulation for the two patches is shown for left-handed circular polarization (LHCP). In Figure 13(b), it can be seen graphically how $|E|$ field value decays quicker when using double layer edge-location via EBG structures.

5. Conclusion

This paper presents and proposes a combination of double layer and edge-location via techniques for EBG size reduction. With these techniques, a 30% of size reduction in comparison to the original mushroom shapes is achieved. This F shape mushrooms maintain the broad bandwidth operation, and these are used in order to suppress the surface wave modes and consequently to reduce the mutual coupling between radiating elements in low-permittivity substrates.

Acknowledgments

The simulations contained in this work have been carried out using CST Microwave Studio Suite 2011 under a cooperation agreement between Computer Simulation Technology (CST) and Universidad Politécnica de Madrid. The authors kindly thank the company NELTEC S.A. for giving samples of the substrates, in which the prototypes were built. This work has been supported by a UPM Grant no. CH/003/2011 and the sicomoro project with Reference no. TEC2011-28789-C02-01.

References

[1] M. A. Salas-Natera, A. García-Aguilar, J. Mora-Cuevas et al., *Satellite Communications*, InTech, 2011.

[2] J. R. James and P. S. Hall, *Handbook of Microstrip Antennas*, IEEE Waves Series, 1989.

[3] R. J. Mailloux, "On the use of metallized cavities in printed slot arrays with dielectric substrates," *IEEE Transactions on Antennas and Propagation*, vol. AP-35, no. 5, pp. 477–487, 1987.

[4] C. A. Balanis, *Antenna Theory, Analysis and Design*, Wiley, 3rd edition, 1997.

[5] B. Preetham Kumar, "Design of unequally spaced arrays for performance improvement," *IEEE Transactions on Antennas and Propagation*, vol. 47, no. 3, pp. 511–523, 1999.

[6] M. Salehi, A. Motevasselian, A. Tavakoli, and T. Heidari, "Mutual coupling reduction of microstrip antennas using defected ground structure," in *Proceedings of the 10th IEEE Singapore International Conference on Communications Systems (ICCS '06)*, Singapore, November 2006.

[7] F. Yang and Y. Rahmat-Samii, "Microstrip antennas integrated with Electromagnetic Band-Gap (EBG) structures: a low mutual coupling design for array applications," *IEEE Transactions on Antennas and Propagation*, vol. 51, no. 10, pp. 2936–2946, 2003.

[8] E. Rajo-Iglesias, O. Quevedo-Teruel, and L. Inclán-Sánchez, "Mutual coupling reduction in patch antenna arrays by using a planar EBG structure and a multilayer dielectric substrate," *IEEE Transactions on Antennas and Propagation*, vol. 56, no. 6, pp. 1648–1655, 2008.

[9] E. Rajo-Iglesias, L. Inclan-Sanchez, J. L. Vazquez-Roy, and E. Garcia- Muñoz, "Size reduction of mushroom-type EBG surfaces by using edge-located vias," *Microwave and Wireless Components Letters, IEEE*, vol. 17, no. 9, pp. 670–672, 2007.

[10] L. Yang, M. Fan, F. Chen, J. She, and Z. Feng, "A novel compact electromagnetic-bandgap (EBG) structure and its applications for microwave circuits," *IEEE Transactions on Microwave Theory and Techniques*, vol. 53, no. 1, pp. 183–189, 2005.

[11] E. Rajo-Iglesias, M. Caiazzo, L. Inclan-Sanchez, and P.-S. Kildal, "Comparison of bandgaps of mushroom-type EBG surface and corrugated and strip-type soft surfaces," *Microwaves, Antennas Propagation, IET*, vol. 1, no. 1, pp. 184–189, 2007.

[12] E. Rajo-Iglesias, O. Quevedo-Teruel, and L. Inclán-Sánchez, "Planar soft surfaces and their application to mutual coupling reduction," *IEEE Transactions on Antennas and Propagation*, vol. 57, no. 12, pp. 3852–3859, 2009.

[13] S. Quevedo-Teruel, L. Inclan-Sanchez, and E. Rajo-Iglesias, "Soft surfaces for reducing mutual coupling between loaded PIFA antennas," *IEEE Antennas and Wireless Propagation Letters*, vol. 9, pp. 91–94, 2010.

[14] E. Rajo-Iglesias, J. L. Vázquez-Roy, O. Quevedo-Teruel, and L. Inclán-Sánchez, "Dual band planar soft surfaces," *IET Microwaves, Antennas and Propagation*, vol. 3, no. 5, pp. 742–748, 2009.

[15] L. Inclan-Sanchez, J. L. Vaquez-Roy, and E. Rajo-Iglesias, "High isolation proximity coupled multilayer patch antenna for dual-frequency operation," *IEEE Transactions on Antennas and Propagation*, vol. 56, no. 4, pp. 1180–1183, 2008.

[16] F. Yang and Y. Rahmat-Samii, "Polarization-dependent electromagnetic band gap (PDEBG) structures: designs and applications," *Microwave and Optical Technology Letters*, vol. 41, no. 6, pp. 439–444, 2004.

[17] D. Sievenpiper, L. Zhang, R. F. Jimenez Broas, N. G. Alexöpolous, and E. Yablonovitch, "High-impedance electromagnetic surfaces with a forbidden frequency band," *IEEE Transactions on Microwave Theory and Techniques*, vol. 47, no. 11, pp. 2059–2074, 1999.

[18] C. Caloz and T. Itoh, *Electromagnetic Metamaterials: Transmission Line Theory and Microwave Applications: The Engineering Approach*, John Wiley and Sons, 2006.

[19] F. Yang and Y. Rahmat-Samii, *Electromagnetic Band Gap Structures in Antenna Engineering*, The Cambridge RF and Microwave Engineering Series, 2008.

[20] P.-S. Kildal, "Definition of artificially soft and hard surfaces for electromagnetic waves," *Electronics Letters*, vol. 24, no. 3, pp. 168–170, 1988.